TRANSITION PHENOMENA IN THE THIOPHENE CRYSTAL *

NORIMARU OKAMOTO **, MASAHARU OGUNI *** and HIROSHI SUGA

*Department of Chemistry and Microcalorimetry Research Center, Faculty of Science,
Osaka University, Toyonaka, Osaka 560 (Japan)*

(Received 7 October 1989)

ABSTRACT

Heat capacities of thiophene–benzene binary solutions $[(1-x)C_4H_4S + xC_6H_6]$ with $x = 0.199$, 0.404 and 0.601 were measured by an adiabatic calorimeter in the temperature range 13–300 K. The results are presented in the form of phase diagrams in the thiophene-rich region and over the whole concentration range. The change in temperature, size, and shape of the heat capacity anomalies occasioned by the composition variation indicated that, for this system, changes in molecular environment exerted considerable effects on the phase and glass transitions of pure thiophene. Calculated solidus and liquidus lines based on Raoult's law showed that a considerable deviation from ideal mixing occurred in either or both of the solid and liquid solutions. The calorimetric entropy of each solid solution was calculated to derive a possible residual entropy arising from frozen-in processes in the system.

INTRODUCTION

As is well known, scientific knowledge is generally based on our limited observation of experiment which is undertaken in laboratory time. Practically all the chemical thermodynamic equilibria are pseudo-equilibria in the sense that it is not the absolute minima of Gibbs energy with respect to all possible processes but only with respect to processes which could take place within a reasonable time.

Orientational ordering processes in many disordered crystals [1] cannot escape from this situation. The ordering process is sometimes interrupted by a freezing-in process (glass transition phenomenon in a broad sense) before

---

* Contribution No. 4 from the Microcalorimetry Research Center. Presented at the International Conference on Chemical Thermodynamics and Calorimetry, Beijing, P.R. China, 25–28 August 1989.
** Present address: Central Research Laboratories, Idemitsu Kosan Co. Ltd., Sodegaura Kami-izumi, Kimitsu-gun, Chiba 299-02, Japan.
*** Present address: Department of Chemistry, Faculty of Science, Tokyo Institute of Technology, O-okayama, Meguro-ku, Tokyo 152, Japan

the crystal reaches an equilibrium ordered state that accords with the third law of thermodynamics. This kind of freezing process has been typically observed in ice [2] and CO [3] crystals and the name "glassy crystals" [4] was given to those possessing some frozen-in orientational degrees of freedom. The corresponding residual entropy was used to argue the nature of the remaining disorder persisting in the crystal. Thus the phase and glass transitions are the phenomena encountered in a continuous cooling of disordered crystals, depending on the relative magnitude of the ordering energy compared with the activation energy required for the re-orientational motion to take place.

Thiophene, a heterocyclic five-membered molecule, is known to crystallize into an orthorhombic system [5] which is the same as that of benzene having six-fold symmetry [6]. This means that significant orientational disorder exists in the thiophene crystal. In fact, thiophene exhibits a variety of phase and glass transitions. The corresponding entropy associated with the orientational degree of freedom of the molecule is removed stepwise through a sequence of phase transitions.

In the present paper, we first describe briefly the phase relation of pure thiophene crystals clarified by the previous experiment. Some of the contradicting observations led us to undertake a series of calorimetric measurements on the thiophene–benzene binary system [7]. Th measurements are based on the fact that both components are mutually miscible not only in the liquid but also in the solid [8]. In the second part, the phase diagram of the system in the thiophene-rich region is reviewed, focussing attention on a peculiar dependence of a particular phase transition of thiophene on the benzene concentration. Finally, the phase diagram in the whole range of x is presented based on new calorimetric measurements.

Generally, adiabatic calorimetry is a powerful and unique method for clarifying the entropy aspect of disordered systems. However, calorimetric studies on two-component systems [9] are quite a few in number. This may be partly due to the unfailing patience required for the preparation of uniform solid solutions, and partly to the subsequent time-consuming and laborious measurements of heat capacities for several samples with different compositions. These experimental difficulties were overcome by the construction of an on-line automated adiabatic calorimeter [10].

EXPERIMENTAL

Thiophene and benzene were taken from the same purified lots used in the previous study [7]. Both of the component liquids were mixed in vacuo to produce ten kinds of solution. Each solution was prepared by weighing the first component in a weighing bottle with a Teflon cock and then adding the second component and reweighing. The amount of benzene remaining in

the purified thiophene as the main impurity was corrected for in determining the final composition of each solution. The sample solution was loaded in vacuo into a gold-plated calorimeter cell of 32.0 cm^3 capacity, and the cell was sealed with a small amount of He gas to facilitate thermal equilibration.

The heat capacity was measured by a low-temperature adiabatic calorimeter with a built-in cryorefrigerator [10] and a fully automated data acquisition system [11]. A Leed and Northrup capsule-type platinum resistance thermometer was used for all temperature determinations. The measurement was made with the intermittent heating mode under adiabatic conditions. Generally, a new thermal equilibrium was attained with 3–5 min after a heating period, depending on the temperature range. The initial and final temperatures before and after the energizing period were corrected for the slight quasi-adiabaticity of the system by extrapolating the observed temperature drifts to the mid-point of the energy input period. Equilibration became sluggish during the transition and melting processes. In such cases, the temperature measured at 5 ks after an energy input was regarded as the new equilibrium temperature.

Special care was taken to obtain a sample of solid solution as homogeneous as possible. Each solution was crystallized quickly in a supercooled liquid state and then annealed at a temperature just below the solidus line which had been determined in advance. The annealing was continued until any exothermic process due to homogenization of the composition ceased almost completely. The procedure required 2–7 days depending on the composition. A longer time was required for the benzene-rich solution in spite of the fact that it had a higher solidus temperature and hence higher diffusion constant than those of the other side. The longer equilibration time may reflect a wider distribution of composition in the benzene-rich sample prepared in the initial, fast crystallization at a non-equilibrium state.

The apparent heat capacity obtained directly by the experiment was corrected for the vaporization effect inside the calorimetric cell [12]. For this purpose, the vapour pressure data of thiophene and benzene were expressed in the form of the Antoine equation

$$\log(p/\text{mmHg}) = A - \frac{B}{C + (t/^\circ C)} \tag{1}$$

TABLE 1

Amount of substance, m_s, volume of substance, V_s, and the Antoin coefficients A, B, C for the vaporization correction

x	$\dfrac{m_s}{\text{g}}$	$\dfrac{V_s}{\text{cm}^3}$	A	B	C
0.199	29.3592	28.66	6.86	1210	221.2
0.404	23.7823	24.15	6.95	1230	221.1
0.601	27.7964	29.30	6.94	1230	221.0

where A, B and C are constants. The vapour pressures of thiophene–benzene solutions were measured by Triday and Rodriguez [13] at 35, 40 and 45°C. The data were assumed to follow the same equation and the three constants were determined by the least-squares fitting of the data for each solution. Numerical values of the constants are listed in Table 1 along with the amount and volume of each sample.

RESULTS AND DISCUSSION

Phase relation of thiophene

In order to describe the complex behaviour of the thiophene–benzene binary system, it is necessary to start with a brief account of the phase relation of pure thiophene. Waddington et al. [14] were the first to demonstrate that thiophene exhibits four crystalline modifications which were designated I, II, III and IV from the high temperature. Later, André et al. [15] found that the II → I transition was actually composed of two transitions: a higher-order transition followed by a first-order transition on cooling. The intermediate phase was assigned as the new phase II, so that there are five phases in total. They also noticed that the first-order transition was easily avoided by a normal cooling experiment, giving rise to metastable phases (II_1 and II_2) with their own phase transitions. The existence of the metastable-phase sequence was confirmed by our subsequent calorimetric measurements [16]. The results are reproduced in Fig. 1. In the metastable state, we found a first-order phase transition around 90 K, which separates the two metastable phases II_1 and II_2. The sharp heat capacity peak was missed in the previous measurement [15]. Similarity of the heat capacity
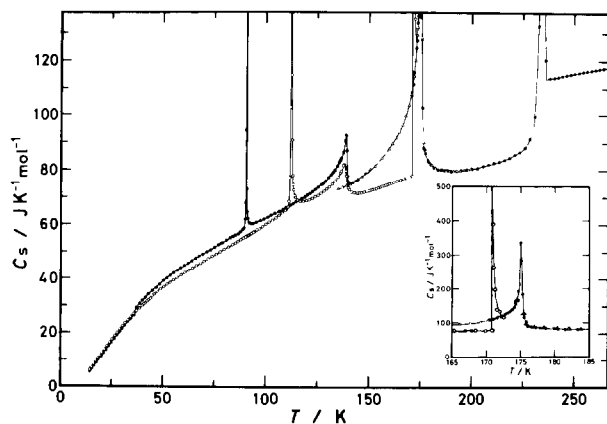

Fig. 1. Molar heat capacity of thiophene in stable and metastable phase sequences.

T/K		112 35	138 5	170 70	175 03	235 03
Phase (stable sequence)	V	IV	III	II	I	Liq
Phase (metastable sequence)	II$_2$	II$_1$				
T/K		90 76	139 2	170 70	175 03	235 02

Fig. 2. Schematic diagram of phase sequence of thiophene.

anomalies associated with the V → IV → III transitions in the stable sequence and the II$_2$ → II$_1$ → II transitions in the metastable sequence is noticeable and this means that similar mechanisms hold for both series of phase transitions.

Both of the lowest temperature phases, V in the stable-phase sequence and II$_2$ in the metastable-phase sequence, were found to exhibit glass transition phenomenon around 45 K for the former and around 37 K for the latter. The calorimetric entropies of both phase sequences compared with the spectroscopic entropy of thiophene showed that residual entropy amounting to (1.25 ± 0.9) J K^{-1} mol^{-1} was retained by phase V and (1.48 ± 0.9) J K^{-1} mol^{-1} by phase II$_2$. Thus thiophene provides a new category of glassy crystals in the sense that both the stable and metastable phases have freezing processes at low temperatures. The phase sequence as clarified by the calorimetric measurement is drawn schematically in Fig. 2.

In what follows, the experimental results of the heat capacity of the thiophene–benzene binary system $[(1 - x)C_4H_4S + xC_6H_6]$ and the phase diagram derived from them are described.

Phase diagram in the region x < 0.03

Although the discovery of the metastable-phase sequence in thiophene has solved some contradictory observations reported in several earlier papers, the unsuccessful observation by André et al. of the first-order heat-capacity peak at 90.76 K raised another problem. The only difference between the two calorimetric measurements was the purity of both samples. Our thiophene sample was purified from a commercial reagent to 99.94%, while they used a high-quality commercial sample without further purification. The main impurity involved in our sample, as revealed by a gas chromatograph, was benzene. In view of the similar chemical properties of benzene and thiophene and their mutual miscibility in liquid as well as in solid, an impurity effect of benzene on the II$_2$ → II$_1$ transition was suspected.

The doping effect of benzene on the phase stability was studied by calorimetric measurement [7] of seven binary solutions with $x = 0.0016$, 0.0030, 0.0050, 0.0061, 0.0070, 0.0183 and 0.0210, respectively. As expected, the transition II$_2$ → II$_1$ disappeared at the mole fraction $x = 0.0070$ of benzene. The results are summarized in Fig. 3 as the partial phase diagram.
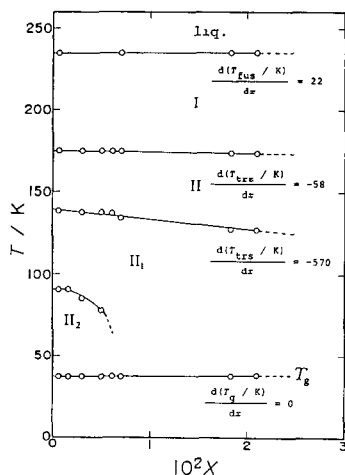
Fig. 3. Phase diagram of the thiophene–benzene binary system in the thiophene-rich region.

For the samples $x = 0.0006$ and 0.0016, the transition exhibited the sharp heat-capacity peak at essentially the same temperature. When x was increased to 0.0030, the transition took place at a temperature 5 K lower than that of the purest sample. The associated heat capacity lost its sharpness dramatically. The anomalous heat capacity was scarcely observed for $x = 0.0050$. At the same time, thermal hysteresis of the transition became prominent. The extent of supercooling of the transition was roughly 2 K for $x = 0.10016$, 11 K for $x = 0.0030$, and 24 K for $x = 0.0050$. For the sample $x = 0.0061$, the $II_1 \rightarrow II_2$ transition happens to take place hypothetically below the glass transition. Obviously this transition is inhibited kinetically. Thus the doping of benzene enhances drastically the stability of phase II_1 and persuades the phase to exist down to the lowest temperature.

The significant effect of benzene on the $II_2 \rightarrow II_1$ transition of thiophene may be related to the incommensurate structures of phases II and II_1 [17]. Both of them correspond to superstructures of the orthorhombic lattice of phase I which constitutes a common geometrical frame with which they are not commensurable. Incommensurate structures are known generally to be affected sensibly by impurities and lattice defects [18] through the pinning effect of the incommensurable modulation wave [19]. Thus the impurities will hinder the incommensurate phase to transform into a commensurate phase upon cooling, leading to freezing of the incommensurably modulated structure. The lock-in transition is known to disappear by a slight doping of particular impurity in the A_2BX_4 family [20].

The other transitions are also affected more or less by the dopant. The melting transition has a positive slope against concentration, while the $II \rightarrow I$ and the $II_1 \rightarrow II$ phase transitions have negative slopes. The glass transition temperature is almost independent of x. For the purest sample,
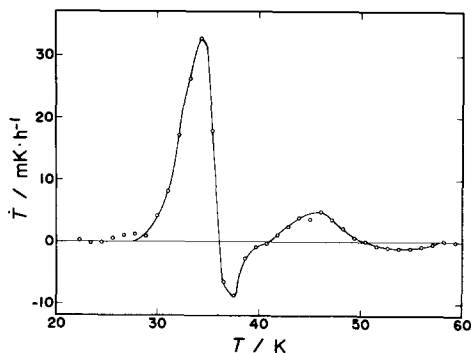
Fig. 4. Anomalous behaviour of the temperature drift rates observed in the solution $(C_4H_4S)_{0.9790}(C_6H_6)_{0.0210}$.

spontaneous positive temperature drifts due to enthalpy relaxation are followed by negative ones, as is observed typically in the glass transition region of a liquid. As the benzene concentration is increased, the behaviour of the enthalpy relaxation becomes complicated. Thus, for the sample $x = 0.0210$, the temperature drift rate plotted as a function of temperature shows that there exists a pair of glass transitions taking place consecutively with temperature. The result is shown in Fig. 4. This means that there are at least two kinds of thiophene molecules in the solid solution which have different environments and hence different kinetic parameters governing the relaxation processes [21]. This effect will be examined by a dielectric measurement in the near future.

Phase diagram over the whole region

All the samples for $x > 0.0210$ realized only the metastable phases. The samples did not show any exothermic process due to the irreversible transformation from the supercooled phase II into the stable phase III even with a long annealing time at around 155 K. Phase III is known to have the normal orthorhombic structure (space group *Pnma*) [22]. Again, this observation gives further evidence of the stabilization of the incommensurate structure of phase II by benzene doping, which hinders the restoration of the normal structure with lower Gibbs energy. This situation compelled us to make the subsequent heat capacity measurements only for the metastable-phase sequence for the samples above that concentration.

Three kinds of solid solution with $x = 0.199$, 0.404 and 0.601 were freshly prepared and their heat capacities were measured in a similar way. Table 2 lists some experimental data for the heat capacity. These are representative data because the entire collection is too large to be accommodated. The quantity corresponds to the molar heat capacity at saturated vapour pressure C_s. The estimated accuracy of the data is 1% below 20 K, 0.3% between 20 and 60 K, and 0.1% above 60 K.

TABLE 2

Representative data of molar heat capacity at saturated vapour pressure, C_s, of $(C_4H_4S)_{0.801}(C_6H_6)_{0.199}$

$\dfrac{T_{av}}{K}$	$\dfrac{C_s}{J\,K^{-1}\,mol^{-1}}$	$\dfrac{T_{av}}{K}$	$\dfrac{C_s}{J\,K^{-1}\,mol^{-1}}$	$\dfrac{T_{av}}{K}$	$\dfrac{C_s}{J\,K^{-1}\,mol^{-1}}$	$\dfrac{T_{av}}{K}$	$\dfrac{C_s}{J\,K^{-1}\,mol^{-1}}$
13.21	5.079	71.54	49.92	154.20	79.46	211.14	82.11
13.86	5.683	72.61	50.37	154.83	79.93	212.87	82.68
14.61	6.380	73.68	50.80	155.46	80.19	214.61	83.91
15.44	7.167	74.75	51.22	156.08	81.01	216.35	83.86
16.35	8.049	75.82	51.65	159.69	81.88	218.09	84.62
17.31	9.014	76.90	52.06	157.30	82.80	219.83	85.46
18.34	10.10	77.98	52.49	157.90	83.75	221.57	86.41
19.03	10.83	79.07	52.90	158.50	84.81	223.31	87.47
19.77	11.59	80.15	53.32	159.98	85.98	225.05	88.92
20.55	12.45	81.24	53.70	159.67	87.22	226.77	90.72
21.36	13.32	82.34	54.10	160.25	88.58	228.48	93.21
22.20	14.20	83.43	54.48	160.83	90.07	230.17	96.88
23.05	15.13	84.53	54.88	161.40	91.66	231.78	103.1
23.92	16.06	85.64	55.26	161.95	93.87	233.32	114.0
24.80	17.00	86.74	55.64	162.50	95.95	234.72	135.2
25.69	17.94	87.85	56.00	163.04	98.38	235.91	179.1
26.59	18.87	88.97	56.39	163.57	101.3	236.82	265.9
27.49	19.80	90.08	56.76	164.10	104.3	237.44	418.1
28.41	20.72	91.21	57.16	164.61	107.2	237.90	691.7
29.33	21.64	92.33	57.51	165.12	110.3	238.24	1073
30.25	22.55	93.46	57.89	165.62	114.1	238.46	1403
31.17	23.45	94.59	58.25	166.11	117.5	238.63	1635
32.10	24.34	95.73	58.62	166.60	121.3	238.77	1885
33.03	25.21	96.87	59.00	167.08	125.1	238.90	2094
33.96	26.07	98.01	59.43	167.55	129.1	239.01	2225
34.90	26.90	99.16	59.83	168.02	133.4	239.13	2250
35.83	27.75	100.31	60.18	168.47	138.3	239.24	2239
36.77	28.58	101.95	60.71	168.91	144.2	239.48	2267
37.71	29.38	103.61	61.22	169.33	151.8	239.62	2274
38.66	30.17	105.28	61.73	169.74	161.7	239.95	2335
39.60	30.94	106.94	62.24	170.17	126.9	240.52	261.3
40.55	31.71	108.61	62.74	170.69	94.44	242.03	116.7
41.50	32.48	110.28	63.28	171.28	88.53	243.98	117.1
42.45	33.20	111.95	63.76	171.89	85.58	245.94	117.4
43.40	33.96	113.63	64.28	172.50	83.73	247.89	117.7
44.35	34.68	115.30	64.79	173.13	82.35	249.83	118.0
45.31	35.41	116.98	65.33	173.77	81.89	251.77	118.3
46.27	36.10	118.66	65.80	174.53	80.69	253.71	118.5
47.22	36.79	120.35	66.39	175.30	80.12	255.64	118.9
48.18	37.47	122.03	66.89	176.07	79.61	257.57	119.3
49.15	38.14	123.72	67.49	176.84	79.19	259.50	119.6

TABLE 2 (continued)

$\dfrac{T_{av}}{K}$	$\dfrac{C_s}{J\,K^{-1}\,mol^{-1}}$	$\dfrac{T_{av}}{K}$	$\dfrac{C_s}{J\,K^{-1}\,mol^{-1}}$	$\dfrac{T_{av}}{K}$	$\dfrac{C_s}{J\,K^{-1}\,mol^{-1}}$	$\dfrac{T_{av}}{K}$	$\dfrac{C_s}{J\,K^{-1}\,mol^{-1}}$
50.11	38.80	125.41	67.99	177.61	78.83	261.42	119.9
51.08	39.44	127.10	68.56	178.38	78.60	263.33	120.1
52.05	40.06	128.79	69.10	179.55	78.13	265.25	120.4
53.02	40.69	130.49	69.70	181.12	77.91	267.15	120.9
53.99	41.31	132.19	70.29	182.70	77.77	272.74	121.8
54.97	41.90	133.88	70.87	184.29	77.66	274.62	121.7
55.95	42.49	135.59	71.51	185.90	77.65	276.51	122.3
56.93	43.14	137.29	72.08	187.51	77.73	278.39	122.5
57.92	43.77	139.00	72.72	189.14	77.84	280.27	122.8
58.91	44.15	140.70	73.36	190.78	77.94	282.15	123.3
59.93	44.71	142.41	74.01	192.42	78.10	284.02	123.7
60.98	45.25	144.12	74.72	194.07	78.48	285.89	124.1
62.03	45.80	145.65	75.24	195.75	78.70	287.76	124.3
63.08	46.31	146.65	75.66	197.43	78.95	289.62	124.5
64.13	46.82	147.66	76.07	199.13	79.17	291.47	124.8
65.18	47.32	148.67	76.48	200.82	79.54	293.32	125.3
66.23	47.78	149.68	76.91	202.53	79.88	295.17	125.7
67.29	48.23	150.70	77.31	204.24	80.29	297.02	126.0
68.35	48.61	151.71	77.75	205.96	80.63	298.86	126.1
69.41	49.02	152.73	78.43	207.68	81.10	300.69	126.6
70.47	49.48	153.55	78.93	209.41	81.59		

Experimental data for the three samples are illustrated graphically in Figs. 5–7. Only the transition II → I and melting are observed in the sample $x = 0.199$. For the sample $x = 0.404$, the heat capacity anomaly associated with the II → I transition becomes obscured in its shape. In this case, the sample was annealed for 4 days at 150–160 K for a possible complete transformation into the low-temperature phase II, after annealing the crystal
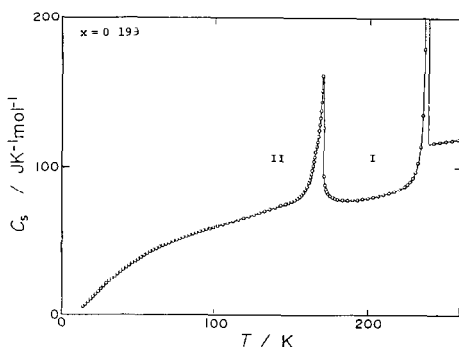

Fig. 5. Molar heat capacity of the binary solution $(C_4H_4S)_{0.801}(C_6H_6)_{0.199}$.
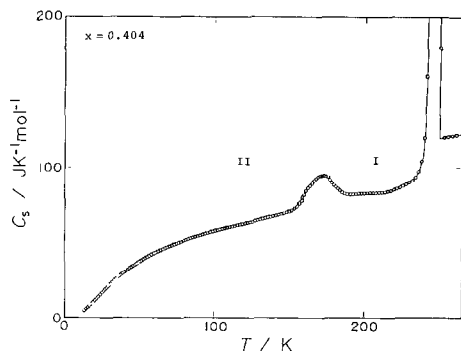
Fig. 6. Molar heat capacity of the binary solution $(C_4H_4S)_{0.596}(C_6H_6)_{0.404}$.

for 5 days just below the solidus temperature for the homogenization of composition. When the benzene concentration is increased to 60.1 mol%, only the fusion process can be observed as shown in Fig. 7. The orientationally disordered phase I continues to persist down to the lowest temperature by heavy doping. The solidus and liquidus temperatures are clearly observed as shown in the inset. The solidus temperature was taken as the intersection of the base line and the steeply rising part of the heat capacities.

Standard thermodynamic functions were calculated based on the pertinent calorimetric data. Extrapolation of the heat capacity to 0 K was carried out by using a 6th-order polynomial function fitted to the experimental data between 13 and 30 K. The functions are typically represented in Table 3 for the sample $x = 0.199$. The corresponding entropy data is depicted graphically in Fig. 8 as a function of temperature. Contributions from nuclear spin, isotope mixing, and possible zero-point entropy are not included in the values. The phase diagram for the system is drawn in Fig. 9 on the basis of the calorimetric data.
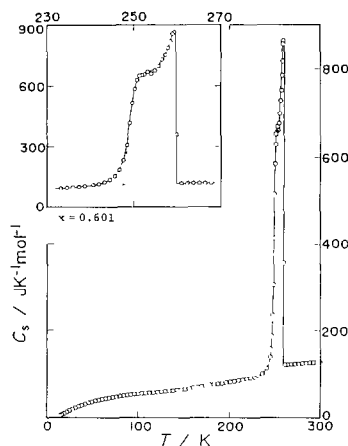

Fig. 7. Molar heat capacity of the binary solution $(C_4H_4S)_{0.399}(C_6H_6)_{0.601}$.

TABLE 3

Thermodynamic functions of $(C_4H_4S)_{0.801}(C_6H_6)_{0.199}$

$\dfrac{T}{K}$	$\dfrac{H(T)-H(0)}{kJ\ mol^{-1}}$	$\dfrac{S(T)-S(0)}{J\ K^{-1}\ mol^{-1}}$
0	0	0
10	0.00700	0.9229
20	0.07570	5.326
30	0.2473	12.14
40	0.5166	19.83
50	0.8678	27.63
60	1.287	35.25
70	1.758	42.51
80	2.271	49.35
90	2.821	55.83
100	3.405	61.98
110	4.022	67.85
120	4.669	73.48
130	5.348	78.91
140	6.061	84.20
150	6.811	89.37
160	7.654	94.80
170	8.835	101.9
180	9.673	106.7
190	10.45	111.0
200	11.24	115.0
210	12.04	118.9
220	12.88	122.8
230	13.77	126.8
240	20.07	153.2
250	21.24	158.0
260	22.43	162.6
270	23.63	167.2
280	24.85	171.6
290	26.09	176.0
300	27.34	180.2
273.15	24.01	168.6
298.15	27.11	179.4

Although such temperature–composition diagrams are usually obtained from thermo-analytical studies, the method is not applicable because the large supercooling effects and the long periods of time required for the present system to attain thermal equilibrium in the transition region obscured the appearance of transitions and caused irreproducibility in cooling curve determinations. Using the adiabatic calorimeter, not only the transition temperature but also the associated enthalpy change were accurately determined. The glass transition in the heavily doped sample becomes complicated. Temperature drifts due to the enthalpy relaxation are found to
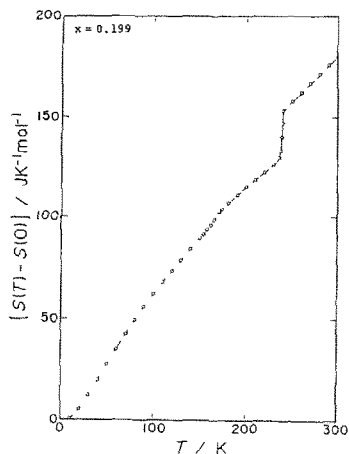
Fig. 8. Molar entropy of the binary system $(C_4H_4S)_{0.801}(C_6H_6)_{0.199}$.

occur from 20 K and continue over a wide range of temperature up to 40 K for the sample $x = 0.199$. The anomalous temperature range widens from 13 and 40 K for $x = 0.601$ and the concept of glass transition temperature becomes unclear. In all cases, the temperature drifts were treated in the heat capacity calculation as if they arise from natural heat leakage, so that the result obtained is equivalent to the "instantaneous" heat capacity without involving the contribution from the relaxational degrees of freedom.

The phase diagram shown in Fig. 9 corresponds to one in which there is complete solid miscibility without any intermediate maximum or minimum in the whole composition range. The formation of the complete solid solution arises from the fact that both of the end members have the same
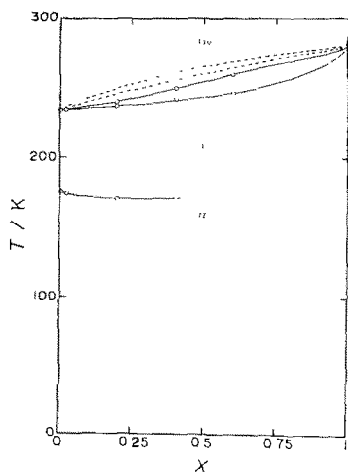

Fig. 9. Phase diagram of the thiophene–benzene binary system.

crystal symmetry and similar lattice constants in the solid phases [23]. The extreme left-hand side of the diagram was already represented in Fig. 3 in an expanded scale. Only the II → I transition can be observed in this scale of composition and the phase boundary between phases II and I disappears above some critical concentration, which should exist between $x = 0.404$ and 0.601.

This is in good contrast to the cases of KCN–KBr [24] and other binary systems [25] in which one component crystal exhibits orientational order–disorder transition. The replacement of the orientationally anisotropic molecules with the second isotropic species lowers significantly the temperature of the ordering transition and leads ultimately to a frozen-in state of the orientational disorder above some critical concentration. Some aspects pertaining to the low-temperature orientational disorder in dilute molecular systems have been reviewed by Binder et al. [26]. The present II → I transition has a characteristic feature in that the transition temperature changes slightly with ever-decreasing entropy of transition by the replacement of thiophene with benzene. The situation is due to the fact that both thiophene and benzene molecules have a one-dimensional rotational degree of freedom around the axes perpendicular to their molecular planes with similar kinetic parameters [27]. Reorientational motion of thiophene molecules results in a distinguishable configuration in the crystal, while that of benzene is neutral in the entropy aspect. Only the symmetry difference in the component molecules will be crucial in determining the behavior of the II → I transition in the binary solution.

A problem of theoretical and practical interest is that of calculating the compositions of the equilibrium liquid and solid solutions at any temperatures where they co-exist. Thermodynamic expressions [28] were derived based on some assumptions. The broken lines in Fig. 9 are the calculated curves based on the models that both of the solid and liquid phases obey Raoult's law and that the enthalpies of fusion are independent of temperature. The latter assumption is not appropriate, especially to the thiophene crystal in which fusion is accompanied by a rather large heat-capacity increase. The doubly concave nature of the calculated curves relative to the composition axis is due to the fact that the enthalpy of fusion of benzene amounts to almost twice that of thiophene, whose fusion temperature is 43 K lower than that of benzene. The large disagreement between the calculated and experimental curves shows significant deviation of the solutions from ideal mixing. One evidence of the deviation from the ideal behaviour can be observed typically in the variation of the enthalpy of fusion with respect to composition, as shown in Fig. 10. Here, the filled circles represent the entropy of fusion and the open circles the enthalpy of fusion. Both of them deviate from the broken lines connecting the values of the end members. The variation of the enthalpy of fusion from the straight line is in the opposite direction to that expected from the actual heat capacity
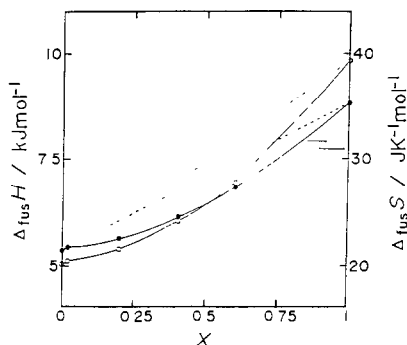
Fig. 10. Molar enthalpy and entropy of fusion of the binary system $[(1-x)C_4H_4S + xC_6H_6]$.

differences of both components between their solid and liquid phases, and indicate clearly the existence of excess enthalpy of mixing in either or both of the solutions.

In pure thiophene crystals, disorder associated with the orientational degree of freedom of the constituting molecules has been removed stepwise through the various phase transitions in both of the phase sequences. As to the metastable-phase sequence, a glass transition occurring around 37 K hinders the crystal from reaching a completely ordered state. The residual entropy of (1.48 ± 0.9) J K^{-1} mol^{-1} corresponding to the freezing process was calculated from a comparison of the calorimetric and spectroscopic entropies [16]. Various phase transitions in the metastable sequence disappears progressively with the increased benzene concentration, and ultimately the high-temperature disorderd phase persists down to the lowest temperature. It is interesting to examine how the residual entropy will change with the amount of benzene.

Figure 11 gives the variation of the entropy at 298.15 K minus that at 0 K, i.e. the calorimetric entropy, of each liquid specimen plotted as a function
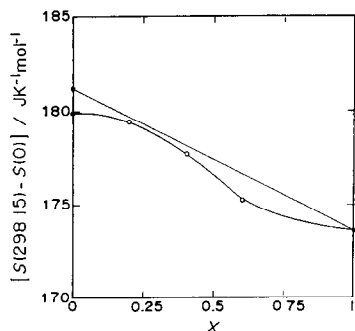

Fig. 11. Calorimetric entropy of the thiophene–benzene binary system calculated at 298.15 K as a function of x.

of mole fraction of benzene (open circles). The filled circles represent the absolute entropies of liquid thiophene and benzene at 298.15 K reckoned backward from their spectroscopic entropies and entropies of vaporization. The difference between the straight line and the calorimetric entropy constitutes a part of the residual entropy of each solid solution. Furthermore we must add the corresponding entropy of mixing of both liquids to the straight line. Again we must face the problem of excess thermodynamic quantities associated with the mixing. The entropy of mixing in a liquid can be obtained in principle by the simultaneous measurements of the vapour pressures and the enthalpies of mixing of the binary solutions over the whole composition. According to Takagi and Kimura [29], both of the excess Gibbs energy and the enthalpy of mixing are small in magnitude in the solutions at 298.15 K. Combination of their data to the present results enables us to calculate the amount of residual entropy as a function of x. Valuable information on the excess thermodynamic quantities of the solid solution will emerge from a careful analysis of the melting equilibrium curves combined with the above data. These calculations will be done in due time.

CONCLUDING REMARKS

It is worth considering generally an impurity effect on the phase transition under conditions of low concentration. In the case of hexagonal ice, trace amounts of alkali hydroxides doped into the ice lattice induced a first-order phase transition at 72 K to produce a proton-ordered phase, ice XI, in an otherwise frozen-in system [30]. A substantial fraction of the residual entropy, which has been accepted as indicative of the frozen-in configurational degree of freedom of protons in ice crystals, was removed by the transition for the specimen doped with KOH in the order of 10^{-3} mole fraction. The dopant is considered to create a pair of ionic and orientational defects which infringe the ice condition governing the rearrangement of proton configuration or water re-orientation in pure ice [31]. The local removal of the motional constraint by the impurity drastically increases [32] the re-orientational motion of all the molecules in the lattice to reveal the phase transition as an intrinsic property of ice, which has been concealed for the kinetic reason [33]. This kind of accelerating effect of the relaxational process induced by impurities has been known in many systems. Thus, for example, the spin–lattice relaxation time of cerium magnesium nitrate hydrate [34] and the conversion rate of nuclear spin in methane [35] were shortened by some paramagnetic impurities.

The situation is in good contrast to the present system in which one of the phase transitions in thiophene, the $II_2 \rightarrow II_1$ transition, disappears by slight doping of benzene in the order of 6×10^{-3} mole fraction. The role of

benzene is to enhance the stability of the phase II_1 and to freeze the incommensurate structure down to the lowest temperature, probably through pinning of the incommensurate modulation waves by the impurity. In this way, phase II_1 is forced to persist without restoring the translational lattice periodicity.

Thus the particular impurity induces the new first-order phase transition in an otherwise frozen system in one case, and another impurity erases the first-order phase transition in an otherwise equilibrium system in another case even in low amounts. Clarification of the role of each dopant on a particular thermal property will deepen our understanding of matter. Chemistry has been developed so far by inventing a new extraction method of pure component from a complicated mixture, by measuring quantitatively various properties of the component, and by expressing the experimental results in a logical way. The number of pure compounds that have been registered so far amounts to ten million. Now we reached a stage where a pure compound should be mixed with a second compound in a controlled way. The second component might hopefully modify the thermodynamic nature of the first component in converting it from an equilibrium to a non-equilibrium state and vice versa. Thus the chemistry of a well-characterized admixture is undoubtedly a new pathway to enrich our world of materials science.

REFERENCES

1 N.G. Parsonage and L.A.K. Staveley, Disorder in Crystals, Oxford University Press, Oxford, 1978.
2 J.W. Stout and W.F. Giauque, J. Am. Chem. Soc., 58 (1936) 1144.
3 J.O. Clayton and W.F. Giauque, J. Am. Chem. Soc., 54 (1932) 2610.
4 H. Suga and S. Seki, J. Non-Cryst. Solids, 16 (1974) 171.
5 S.C. Abraham and W.N. Lipscomb, Acta Crystallogr., 5 (1952) 93.
6 E.G. Cox and J.A.B. Smith, Nature (London), 75 (1954) 173.
7 N. Okamoto, M. Oguni and H. Suga, Solid State Commun., 70 (1989) 219.
8 F.S Fawcett and H.E. Rasmussen, J. Am. Chem. Soc., 67 (1945) 1705.
9 The following references are not exhaustive. H.L. Fink, M.R. Cines, F.E. Frey and J.G. Aston, J. Am. Chem. Soc., 69 (1947) 1501. J.E. Spice, G.A. Harrow, C.R. McGowan and E.B. Smith, Pure Appl. Chem., 2 (1961) 303. E.T. Chang and E.F. Westrum, Jr., J. Phys. Chem., 74 (1970) 2528. J.C. van Miltenburg and H.A.J. Oonk, Mol. Cryst. Liq. Cryst., 28 (1974) 167.
10 K. Moriya, T. Matsuo and H. Suga, J. Chem. Thermodyn., 14 (1982) 1143.

11 K. Kishimoto, H. Suga and S. Seki, Bull. Chem. Soc. Jpn., 53 (1980) 2748.

12 J.P. McCullough and D.W. Scott, Experimental Thermodynamics, Vol. 1, Butterworths, London, 1968.

13 J.O. Triday and P. Rodriguez, J. Chem. Eng. Data, 30 (1985) 112.

14 G. Waddington, J.W. Knowlton, D.W. Scott, G.D. Oliver, S.S. Todd, W.N. Hubbard, J.C. Smith and H.M. Huffman, J. Am. Chem. Soc., 71 (1949) 797.

15 D. André, A. Dworkin, P. Figuière, A. Fuchs and H. Szwarc, C.R. Acad. Sci. Ser. II, 295 (1982) 145; J. Phys. Chem. Solids, 46 (1985) 505.

16 P. Figuière, H. Szwarc, M. Oguni and H. Suga, J. Chem. Thermodyn., 67 (1985) 949.

17 D. André and H. Szwarc, J. Phys. Paris, 47 (1978) 61.

18 R. Blinc and A.P. Levanyuk(Eds.), Incommensurate Phases in Dielectrics, Vols. I and II, North-Holland, Amsterdam, 1986.

19 W.L. McMillan, Phys. Rev. B, 12 (1975) 1187; 14 (1976) 1496.

20 K. Hamano, Y. Ikeda, T. Fujimoto, K. Ema and S. Hirotsu, J. Phys. Soc. Jpn., 49 (1980) 2278.

21 N. Okamoto, M. Oguni and H. Suga, J. Phys. Chem. Solids, 50 (1989) 1285.

22 D. André, P. Figuière, R. Fourme, M. Ghelfenstein, D. Labarre and H. Szwarc, J. Phys. Chem. Solids, 45 (1984) 299.

23 A.I. Kitaigorodsky, Mixed Crystals, Springer-Verlag, Berlin, 1984.

24 A. Loidl, R. Feile and D. Knorr, Z. Phys., B42 (1981) 143.

25 W. Press, B. Janik and H. Grimm, Z. Phys., B49 (1982) 9.

26 K. Binder, W. Kinzel and S. Sarbach, Faraday Discuss. Chem. Soc., 69 (1980) 261.

27 J.E. Anderson, Mol. Cryst. Liq. Cryst., 11 (1970) 343.

28 A. Reisman, Phase Equilibria, Academic Press, New York, 1970.

29 S. Takagi and T. Kimura, private communication, 1990.

30 Y. Tajima, T. Matsuo and H. Suga, Nature (London), 299 (1982) 810.

31 D. Eisenberg and W. Kauzmann, The Structure and Properties of Water, Clarendon Press, Oxford, 1969.

32 S. Kawada, I. Takei and H. Abe, J. Phys. Soc. Jpn., 58 (1989) 54.

33 W. Kauzmann, Chem. Rev., 43 (1948) 219.

34 K.W. Mess, J. Lubbers, L. Niesen and W. Huiskamp, Physica, 41 (1969) 260.

35 G.J. Vogt and K.S. Pitzer, J. Chem. Thermodyn., 8 (1976) 1011.